AIAA 81-4323

Optimal Two-Phase-Flow Nozzle Configurations at Large Volume Ratios

Gustave Hokenson*
Dynamics Technology, Inc., Torrance, Calif.

A self-consistent methodology for establishing the optimal geometric configuration of two-phase-flow converging-diverging nozzles is developed. The analysis relies on a perturbation of the isentropic, homogeneous, equilibrium (IHE) flow model to establish the area ratio, contour, and length scale of optimally efficient nozzles in the limit of large volume ratios. The IHE limit model predicts the pressure-area relationships with reasonable accuracy and provides a simple analytical representation of the bulk flowfield. This formulation is used in the determination of a nozzle contour which minimizes wall friction losses and an aspect ratio which optimizes the nozzle length in a tradeoff between phase slip and wall friction. These optimization procedures are coupled and, applied iteratively, result in a nozzle configuration which optimally accommodates the effects of wall shear, interphase drag, and pressure gradients. Comparison with experimental data is used to validate the approach within the context of the assumptions which were enforced.

Nomenclature

a = speed of sound
A = cross-sectional area
c = constant in Eq. (7) for δ
C_D = particle drag coefficient
C_f = skin friction coefficient
D_0 = particle scale
D_H = hydraulic diameter
E = Euler number, $p/\rho u^{*2}$
f,g,h,I = functions defined in Eq. (7)
J = generalized integrand
k_1 = constant in Eq. (8), $2\,C_f^*(L/D_H^*)$
k_2 = constant in Eq. (8), $3\,C_D(L/D_0)/4$
L = nozzle length
M = Mach number
p = pressure
r = ratio of liquid to gas mass flow rate
S = nozzle surface area per unit length
u = velocity
u_r = relative velocity, $u_g - u_l$
$\bar{u}$ = bulk velocity
v = volume ratio, $(\rho_l/\rho_g)/r$
We = Weber number, $\rho u^2 D_0/\sigma$
x = streamwise position
β = $M^2 - 1$
δ,ϵ = parameters defined by Eq. (7)
λ_1 = $(u_l/u_r)^*$
λ_2 = $(\rho_g u_r^2/\rho_l u_l^2)^*$
λ_3 = $(p/\rho_l u_l^2)^*$
ρ = density
σ = surface tension
θ = momentum thickness
η = efficiency, $(\bar{u}_e/\bar{u}_{e(\text{isentropic})})^2$

Subscripts

crit = conditions for particle breakup
e = nozzle exit
g = gaseous
l = liquid
0 = initial or reference conditions
t = stagnation conditions

Superscripts

( )* = critical or throat conditions
(~) = normalized by throat conditions or L
(˙) = differentiation with respect to x

Introduction

COMPLICATIONS introduced by multiphase flow to the design of *efficient* converging-diverging nozzles are significant.[1,2] Optimal length scaling (aspect ratio), contouring, and area ratio are sensitive to the detailed bubble growth/particle breakup and dynamics. As discussed in Ref. 3, these phenomena are often complex and not easily modeled. This restricts the utility of large-scale computational algorithms whose *design* predictions are difficult to distill into a compact form. Therefore, an approximate solution which perturbs the isentropic, homogeneous, equilibrium (IHE) flow model was developed to synthesize the optimal nozzle geometry for anisentropic, nonhomogeneous, nonequilibrium situations.

Area Ratio

In the limit of large volume ratio (v_t), and assuming that the density ratio is sufficiently small for the mass ratio to be >1, the IHE model of two-phase flow (see Ref. 4) may be expanded to provide the following approximate relationships:

$$\frac{\rho_l u^2/2}{p_t} = v_t \ell n(p_t/p) \tag{1}$$

and

$$\frac{\rho_l a^2/2}{p_t} = v_t/2 \tag{2}$$

Applying Eq. (1) at the nozzle throat and substituting for a from Eq. (2) results in

$$p^*/p_t = \rho^*/\rho_t = e^{-1/2} \tag{3}$$

Combining Eqs. (1) and (2), the local Mach number may be written

$$M^2 = \ell n(p_t/p)^2 \tag{4}$$

Received Dec. 30, 1980; revision received June 25, 1981.

*Senior Research Scientist. Member AIAA.

Utilizing continuity of mass flow, the local area ratio becomes

$$\tilde{A}^2 = e^{\beta}/(1+\beta) \tag{5}$$

where $\beta \equiv \ell n(p_t/p)^2 - 1$ and, therefore, from Eq. (4) $\beta = M^2 - 1$.

The validity of these formulas may be evaluated by comparison with the results in Refs. 1 and 2 for air/water nozzles operating at $r = 10$ and $p_t/p_e = 35$. Equation (5) predicts full expansion at $\tilde{A}_e = 7.96$, whereas the (suboptimal) pressure contour *design* analysis in Ref. 2 results in $\tilde{A}_e = 7.022$. *Evaluation* mode results were computed in Ref. 1 for identical conditions in an annular nozzle with an approximately linear area distribution in the supersonic region. These computations indicate that sensible expansion ceases at $\tilde{A} = 6.93$ for both 7 and 21 deg divergence angle nozzles. Equation (3) satisfactorily predicts the throat conditions for both sets of data.

This simple IHE limit model provides the framework within which anisentropic, nonhomogeneous, nonequilibrium flow phenomena may be analyzed. Based on the substantiation of Eqs. (3) and (5), analytical representations of the two-phase-flowfield properties allow for the evaluation of two "loss" mechanisms of interest: nozzle wall friction and interphase drag.

It will be shown that optimal contouring based on wall shear minimization is derived as a function of nozzle length scale. In addition, the essence of the interphase dynamics analysis is to optimize the nozzle length scale in a tradeoff between wall friction and phase slip. Inasmuch as the optimal nozzle contour (combined with the IHE pressure-area relationship) is used to provide the bulk flow pressure distribution for the particle dynamics analysis, there is a coupling between the following contouring and length scale estimations. Therefore, although the contouring (via wall shear minimization considerations) and length optimization (via exit bulk velocity maximization—including wall shear, interphase drag, and pressure effects) of the nozzle are carried out separately, they are not independent and the final optimal configuration reflects the integrated effect of all phenomena.

Contouring

In order to establish a nozzle contour which "encourages" the IHE flowfield, an optimization procedure was developed in which the wall friction, integrated over the nozzle surface area, is minimized. This procedure may be compared to the approach in Ref. 2 wherein a specific family of nozzle pressure profiles is selected a priori. The particular profile which provides the maximum exit bulk velocity is assumed to be optimal. These approaches are also to be contrasted with classical wave cancellation contouring of gas flow nozzles.

Applying traditional variational principles to the integral $\int \rho u^2 C_f dS$, the following equation for the cross-sectional area distribution of nozzles (whose shape remains similar throughout) may be derived

$$\tilde{A}\ddot{\tilde{A}} - \dot{\tilde{A}}^2/2 = \frac{gh}{1+2gh}\left\{\frac{d\ell nI}{d\ell n\tilde{A}}\right\}\dot{\tilde{A}} + \left(\frac{g}{g-1}\right)\frac{(h+1)-gh}{1+2gh}\left\{\frac{d\ell nf}{d\ell n\tilde{A}}\right\}\dot{\tilde{A}}^2 \tag{6}$$

where

$$f \equiv \tilde{\rho}\tilde{u}^2\tilde{A}^{1/2}, \quad g \equiv (1+\epsilon\dot{\tilde{A}}^2/\tilde{A}), \quad h \equiv \delta I(\tilde{A})\dot{\tilde{A}}$$

and

$$\epsilon \equiv (4L/D_0)^{-2}, \quad \delta \equiv cE/(L/\theta^*), \quad I \equiv (d\tilde{p}/d\tilde{A})/(\tilde{\rho}\tilde{u}^2) \tag{7}$$

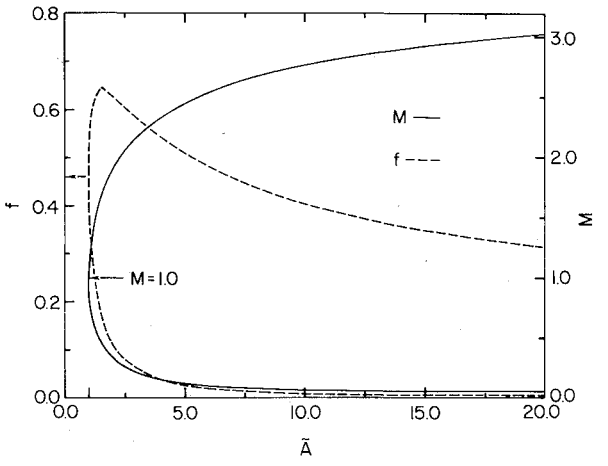

Fig. 1 f **and** M **vs** $\tilde{A}$.

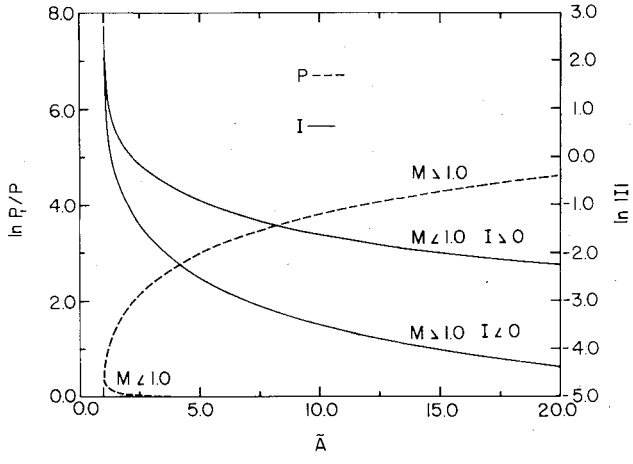

Fig. 2 $\ell n(p_t/p)$ **and** $\ell n\,|I|$ **vs** $\tilde{A}$.

In order to derive Eq. (6), the Euler-Lagrange equation:

$$\frac{d}{d\tilde{x}}\frac{\partial J}{\partial \dot{\tilde{A}}} - \frac{\partial J}{\partial \tilde{A}} = 0 \tag{8}$$

which expresses the minimum value for a definite integral $\int J(\tilde{A}, \dot{\tilde{A}}, \tilde{x})d\tilde{x}$, is applied to $\int \rho u^2 C_f dS$. In this case, $J = fg^{1/2}(1+h)$ where f includes the dynamic pressure and local body radius effect, g accounts for the change in local wetted area due to the angle of the nozzle surface, and h accounts for changes in C_f due to pressure gradients. Note that Eqs. (1-5) allow f and I to be expressed as functions of $\tilde{A}$ and Eqs. (7) convert J to a function of $\tilde{A}$ and $\dot{\tilde{A}}$ with ϵ and δ as parameters in the optimization. These characterize the nozzle aspect ratio and sensitivity of wall friction to pressure gradient, respectively.

Figure 1 presents both subsonic and supersonic branches of f and M as a function of area ratio, with the maximum value of f occurring at $\tilde{A} = 1.65$ and $M = 1.79$. The corresponding results for I and p_t/p are presented in Fig. 2. Given an optimal pressure distribution,[2] the nozzle contour is, therefore, known. However, in this research, the optimal area distribution (for a given length scale) shall be inferred from the solution of Eq. (6) and the resultant implied pressure gradient used to optimize the length scale based on subsequent phase slip considerations.

Phase Dynamics

The IHE limit model and associated optimal nozzle area distribution allow the particle/gas dynamics to be approached

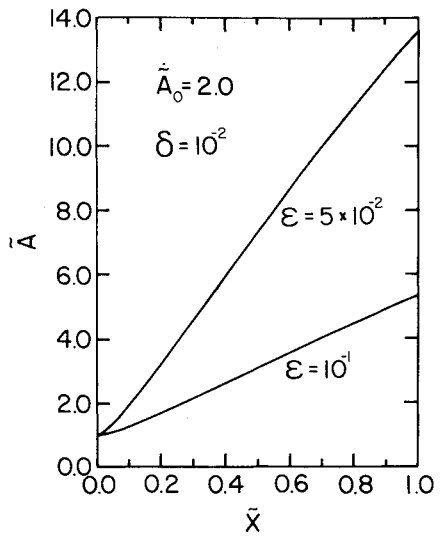

Fig. 3 $\tilde{A}$ vs $\tilde{x}$ for $\dot{A}_0 = 2.0$, $\delta = 10^{-2}$, and $\epsilon = 5 \times 10^{-2}, 10^{-1}$.

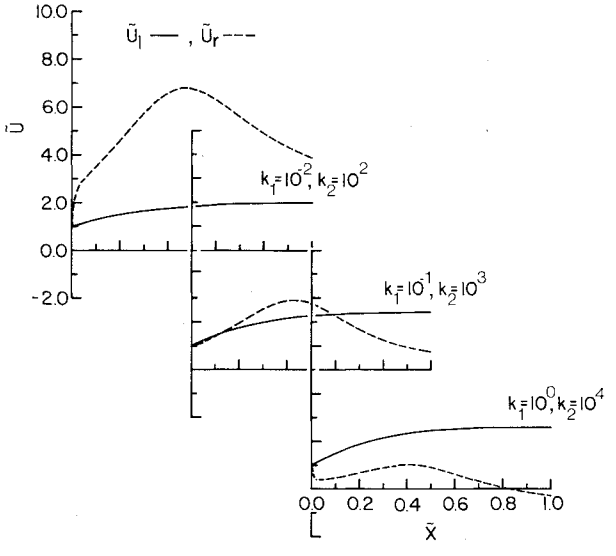

Fig. 4 $\tilde{u}_l$ and $\tilde{u}_r$ vs $\tilde{x}$ for various k_1 and k_2.

in a particularly convenient way, in order to complete the optimization procedure. Under the assumption of high v_t, the IHE pressure-area relationship and optimal area distribution are input to the analysis to provide pressure and area as a function of $\tilde{x}$ for a given nozzle length scale (aspect ratio). In this case, the phase slip and liquid velocities are computed from [1-4]

$$\frac{d\tilde{u}_r}{d\tilde{x}} + \frac{k_1}{\tilde{D}_H}\tilde{u}_r = \mp k_2(1+r)\lambda_1\lambda_2\tilde{p}\frac{\tilde{u}_r^2}{\tilde{u}_l}$$

$$-\frac{k_1\lambda_1}{\tilde{D}_H}\tilde{u}_l - \frac{\lambda_3 d\tilde{p}/d\tilde{x}}{\lambda_2\tilde{p}(\tilde{u}_r + \lambda_1\tilde{u}_l)}$$

$$\tilde{u}_l\frac{d\tilde{u}_l}{d\tilde{x}} = -\lambda_3 d\tilde{p}/d\tilde{x} \pm k_2\lambda_2\tilde{p}\tilde{u}_r^2 \qquad (9)$$

These equations are also dependent upon the various length scales of the problem. Therefore, some iteration with the optimum area distribution is required.

Results

At this point, validation of the approach relies primarily on the data in Ref. 2, wherein two different air/water nozzles were analyzed and tested at $(p_t/p_e) = 35$ with $r = 10$. These nozzles had identical subsonic contraction cones and two different length supersonic sections (7 vs 21 deg divergence angles), with the same overall area ratio. Therefore, the area contour and length optimization developed here will also focus on the supersonic regime. This avoids complex particle breakup dynamics modeling, inasmuch as liquid particulates typically reach a limiting size at the throat. [1,2]

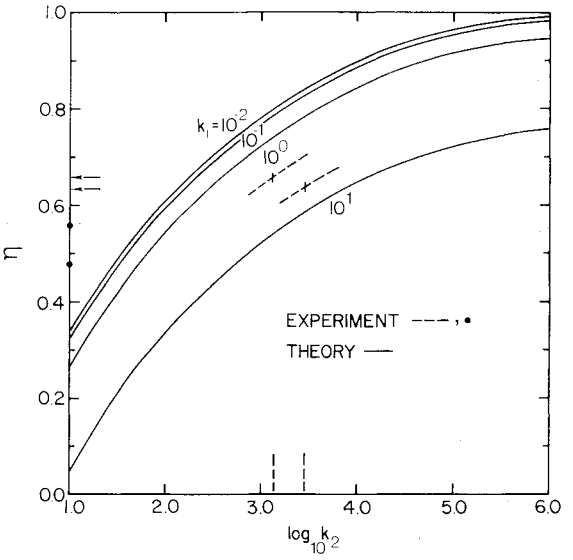

Fig. 5 η vs k_2 for various k_1, compared to the experimental data of Ref. 1.

Given a reliable particle breakup model (e.g., $We = We^{1,2}_{crit}$), the entire nozzle may be computed with the same contour and particle dynamics analysis (utilizing the local particle scale), inasmuch as the IHE pressure-area relationship is applicable to the entire nozzle. For cases of fixed-size particles, the entire nozzle may be computed utilizing these equations without modification.

Typical integration of Eq. (6) from the throat to the exit plane is presented in Fig. 3 and indicates that a simple (nearly) linear area distribution is often optimal. (For axisymmetric nozzles, this results in a configuration approaching a bell shape.) The similarity between these shapes and those in Ref. 2 is remarkable. This, combined with the substantiation of Eqs. (3) and (5) indicates that the information provided in Ref. 2 on the effect of nozzle length should also be relevant to the length scaling optimization procedure developed here.

Note that the solution to Eq. (6) is a split-point boundary value problem. $\tilde{A}_0 = 1$ is required by definition of $\tilde{A}$ and the origin of integration at the throat. Either the subsonic or supersonic nozzle regions may be evaluated, depending on which branch of f and I are chosen as the integration proceeds away from the throat. For a given ϵ and δ, in order to obtain the desired $\tilde{A}_e$, the appropriate $\tilde{A}_0$ is determined iteratively. In lieu of this iteration, the computations may be carried out with $\tilde{A}_0$ as a parameter. A family of nozzle shapes/area ratios is thereby developed.

For a $(p_t/p_e) = 35$ and $r = 10$, the IHE pressure-area relationships are combined with the optimal contour to solve Eqs. (9) and generate profiles of liquid and slip velocities along the nozzle for various values of k_1 and k_2. Typical results are shown in Fig. 4, which illustrate a dependence on nozzle length similar to that presented in Ref. 2. The negative values of $\tilde{u}_r$ shown for $k_1 = 10^0$ and $k_2 = 10^4$ reflect a somewhat nonphysical disparity between C_f and C_D, with the wall shear stress dominating.

It may be shown that the bulk (mass flow-weighted mean) velocity is related to the slip and liquid velocities by

$$\tilde{u} = u_g - ru_r/(1+r) \qquad (10)$$

The measured bulk velocities in Ref. 2 are 170 and 183 m/s for nozzles I (7 deg) and II (21 deg) and resulted in efficiencies (η) of 0.48 and 0.56, respectively. Utilizing Eqs. (9) and (10), the computed nozzle efficiency is plotted in Fig. 5 as a function of k_1 for various k_2. Compared with the data from Ref. 2, it is seen that the trend toward higher efficiency with shorter nozzles is predicted analytically. For these flow conditions, this dependence is observed only for large k_1 nozzles, due here to the small throat hydraulic diameter of annular nozzles.

Conclusion

An approximate, self-consistent procedure has been developed to determine the optimal area ratio, contour, and aspect ratio of two-phase-flow nozzles with large volume ratios. Results of the analysis have been validated by comparison with experimental data obtained from nozzles which closely approximate the computed optimal configuration. At this stage of the analysis, fixed-size particles were considered in the assessment of optimal nozzle aspect ratio. However, given a reliable particle size model for any given situation, the identical procedure may be employed utilizing a variable particle scale.

Acknowledgment

The author would like to acknowledge the assistance of Prof. D.W. Netzer in providing information which was crucial to the evaluation of the analytical results obtained during this research.

References

[1] Warner, C.F. and Netzer, D.W., "An Investigation of the Flow Characteristics of Two-Phase Flow in Converging-Diverging Nozzles," ASME Paper 63-WA-192, Winter Annual Meeting, Philadelphia, Pa., Nov. 1963.

[2] Elliott, D.G. and Weinberg, E., "Acceleration of Liquids in Two-Phase Nozzles," NASA Tech. Rept. 32-987, July 1968.

[3] Clift, R., Grace, J.R., and Weber, M.E., *Bubbles, Drops and Particles,* Academic Press, New York, 1978.

[4] Wallis, G.B., *One-Dimensional Two-Phase Flow,* McGraw-Hill Book Co., New York, 1969.